Lab Notes

Editors
Thomas M. Moses | Shane F. McClure

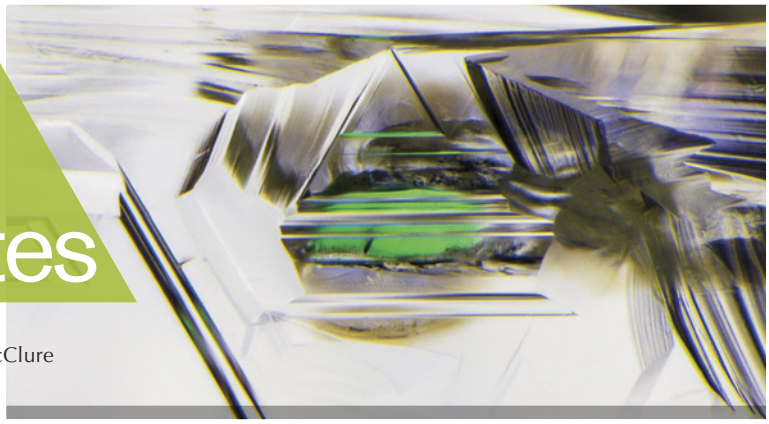

Purple ANHYDRITE

Recently, the Carlsbad laboratory received a 2.13 ct transparent purple octagonal step cut, measuring 7.32 × 6.34 × 6.01 mm (figure 1), for a colored stone identification service. Microscopic observation showed twinning planes, cleavage cracks, needle-like inclusions, fluid fingerprints, and strong doubling of many internal features, confirming the stone was doubly refractive (figure 2).

Standard gemological testing revealed a specific gravity of 2.97 and a refractive index of 1.570–1.615 with a birefringence of 0.045. The refractive index measurement also indicated the stone was biaxial positive, and a biaxial interference figure was resolved using a conoscope and polarized light. Purple and light purple pleochroism was observed using a dichroscope. The specimen had no fluorescence reaction when exposed to long- and short-wave UV light. These characteristics were consistent with the rare collector gem anhydrite.

Raman spectroscopy confirmed that the stone was anhydrite. Using polarized ultraviolet/visible/near-infrared spectroscopy, we were able to determine that the purple color resulted from a prominent absorption band centered at around 550 nm. A sharp absorption feature was also observed at 307 nm.

Figure 1. This 2.13 ct purple stone was identified as the rare collector gem anhydrite.

Anhydrite is a calcium sulfate with the chemical formula $CaSO_4$. It is not well suited for use in jewelry due to its low hardness of 3.5 on the Mohs scale and its perfect cleavage in one direction. This orthorhombic mineral is commonly formed by the dehydration of gypsum, which has the chemical formula $CaSO_4 \cdot 2H_2O$, and can have multiple colors ranging from colorless to pale blue, light pink, and brown that is colored by impurities. Occurrences of purple anhydrite have been reported in Switzerland, Iran, and Sri Lanka (see, respectively, Spring 1998 Gem News, p. 60; Fall 2000 Gem News, p. 262; Fall 1988 Gem News, p. 179).

Faceted gem-quality and single-crystal anhydrite is rare, and while the Carlsbad laboratory has examined a couple of anhydrite gems, they were mostly aggregates bluish in color. This is the first example of a transparent purple faceted single crystal anhydrite examined at GIA's Carlsbad laboratory.

Maria Estela Almeida and Nathan Renfro

Figure 2. Twinning planes and fluid fingerprints were observed throughout the faceted purple anhydrite. Field of view 3.89 mm.

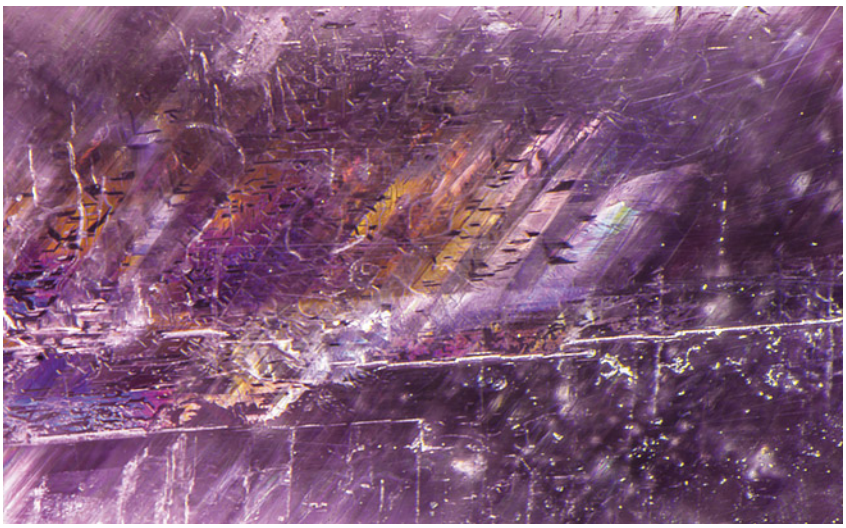

Editors' note: All items were written by staff members of GIA laboratories.

Gems & Gemology, Vol. 59, No. 1, pp. 72–82.

Figure 3. A 7.26 ct modified round brilliant identified as pink pyrope garnet. Courtesy of Bill Vance.

Pink Pyrope GARNET

The Carlsbad laboratory received a 7.26 ct pink modified round brilliant (figure 3) for a colored stone identification report. Standard gemological testing revealed that the stone was singly refractive with a refractive index (RI) of 1.741 and a hydrostatic specific gravity (SG) of 3.77, properties consistent with garnet. Internally the stone was quite clean, with microscopic examination revealing scattered short needles.

The garnet group is composed of more than 20 species, all of them sharing the basic chemical formula $X_3Y_2(SiO_4)_3$. Five of these species are common within the jewelry industry: almandine, andradite, grossular, pyrope, and spessartine. Andradite and grossular are ugrandite garnets; they have calcium in the X site of their chemical formula. Almandine, pyrope, and spessartine are all pyralspite garnets containing aluminum in the Y site. Isomorphous replacement, in which one chemical element substitutes for another in a mineral's crystal structure, makes it possible for garnets to be a chemical mixture of two or more garnet species. GIA gemologists use a garnet's gemological properties and chemistry to categorize the stone into its particular species.

Chemical analysis revealed that the 7.26 ct stone was a pyralspite garnet due to the high aluminum concentration (values expressed in wt.%: MgO 18.50%, Al_2O_3 23.05%, SiO_2 41.32%, CaO 1.89%, TiO_2 0.05%, V_2O_3 0.02%, Cr_2O_3 0.04%, MnO 11.93%, Fe_2O_3 3.17%). The composition of this garnet and its gemological properties were consistent with pyrope, which has an RI of 1.73–1.75, an SG of 3.78 (+0.009/–0.016), and magnesium dominating the X site and minor amounts of manganese and iron. Pyrope garnet, though, has a color range of red to reddish orange and colorless. Pink pyrope garnet is incredibly rare, especially in stones of this size.

Pyrope-spessartine can have a bodycolor similar to pyrope but has an RI range of 1.75 to over the limit and an SG of 3.78, both higher than the values documented for this pink garnet. The fact that garnet can be a mixture of species can make the identification of these stones challenging. This example is an important reminder to carefully analyze a garnet's gemological properties to accurately identify it and how the laboratory can use chemical analyses as validation.

Nicole Ahline

Libyan Desert GLASS Bangle Bracelet

Libyan Desert glass is a light green or yellow natural glass which is composed of almost 98% silica. It is a type of tektite formed by meteorite impact in the desert and the fast quenching of the silica-rich melt produced. It was first reported by Clayton and Spencer in 1934 (F. Fröhlich et al., "Libyan Desert Glass: New field and Fourier transform infrared data," *Meteoritics and Planetary Science*, Vol. 48, No. 12, 2013, pp. 2517–2530) and is found in Egypt's Western Desert. Common inclusions are bubbles, cristobalite, dark brown streaks, and black iron oxides (J.A. Barrat et al., "Geochemistry and origin of Libyan Desert glasses," *Geochimica et Cosmochimica Acta*, Vol. 61, No. 9, 1997, pp. 1953–1959).

Recently, GIA's Hong Kong laboratory examined a transparent light yellow bangle bracelet measuring 66.12 × 13.10 mm and weighing 144.67 ct (figure 4). It had a spot refractive index of 1.44 and revealed weak yellow fluorescence in shortwave UV. The chemical composition, determined by qualitative analysis using energy-dispersive X-ray fluorescence, was nearly pure silica with

Figure 4. A 144.67 ct Libyan Desert glass bangle measuring 66.12 × 13.10 mm.

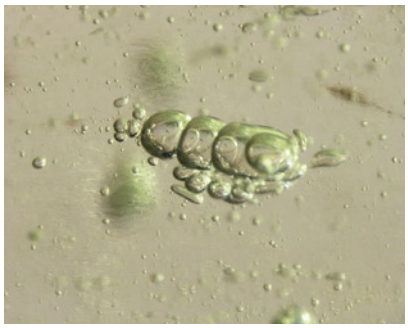

Figure 5. Various shapes of gas bubbles were dispersed individually and in clusters in the Libyan Desert glass bangle. The row of gas bubbles in this image resembles peas in a pod. Field of view 2.40 mm.

minor amounts of iron, strontium, potassium, titanium, and zirconium.

Based on the differences in molecular vibrations detected with Fourier-transform infrared (FTIR) analysis, it was determined that the molecular structure of Libyan Desert glass is significantly different from that of other pure silica glasses. It has a higher ratio of discontinuities and defects in the tetrahedral (SiO_4) network (F. Fröhlich et al., 2013). Microscopic observation revealed common inclusions in glass such as numerous gas bubbles (figure 5) and flow structure. This bangle also presented abundant white spherulites identified by Raman spectroscopy as cristobalite (a polymorph of silica). These spherulites were small and individually dispersed throughout the glass (figure 6). The presence of this high-temperature low-pressure silica phase indicates a natural high-temperature formation. From all the gemological, FTIR, and Raman data collected, this bangle was identified as Libyan Desert glass.

Figure 6. White spherulites in the bangle were identified as cristobalite by Raman analysis. Field of view 5.98 mm.

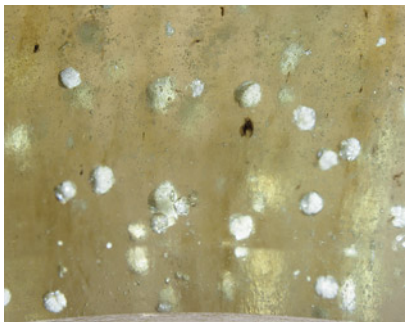

Most Libyan Desert glass is tubular in shape, and some are approximately spherical or rod-like (R.A. Weeks et al., "Libyan Desert glass: A review," *Journal of Non-Crystalline Solids*, Vol. 67, No. 1-3, 1984, pp. 593–619). Those fragments are usually 2 to 63 mm in size, so it is surprising to examine this material in the form of a bangle bracelet.

Ching Yin Sin

PEARLS

"Atypical Beads": Variations of Two Types of Nuclei

Atypical bead cultured pearls (aBCP) are occasionally encountered during laboratory testing. The nuclei used can take the form of various undrilled, partially drilled, or even drilled materials including natural pearls (abalone, scallop, turban species, *Pteria* species, and *Pinna* species), freshwater non-bead cultured pearls, coral, plastic, small shells, faceted sapphire beads of various colors, glass, quartz, and agate ("Atypical 'beading' in the production of cultured pearls from Australian *Pinctada maxima*," *GIA Research News*, February 13, 2017). Four aBCPs (figure 7) were recently discovered in a group of 50 loose pearls submitted to GIA's Mumbai laboratory.

Externally, the four white to light cream-colored aBCPs looked similar to the other pearls submitted in the lot. When viewed under 40× magnification, their surfaces exhibited a typical nacreous surface of overlapping aragonite platelets. Energy-dispersive X-ray fluorescence spectrometry on all four revealed manganese levels between 13.30 ppm and 45.60 ppm and strontium levels between 1064 ppm and 1822 ppm, characteristic of a saltwater environment. Interestingly, optical X-ray fluorescence (XRF) of pearl 1 revealed a strong yellowish green reaction, while pearls 2, 3, and 4 were inert. The ultraviolet/visible reflectance spectra collected on the four pearls showed weak absorption features at around 320–420 nm. Raman analysis using 514 nm laser excitation showed the expected doublet at 702/705 cm^{-1} and peak at 1085 cm^{-1}, indicative of aragonite.

Real-time microradiography (RTX) and X-ray computed microtomography (μ-CT) analysis revealed a variety of internal structures that required interpretation. RTX imaging of pearl 1 showed a thin irregular demarcation close to

Figure 7. Four loose atypical bead cultured pearls weighing 3.30 to 8.53 ct. Pearls 1–4 are shown from left to right.

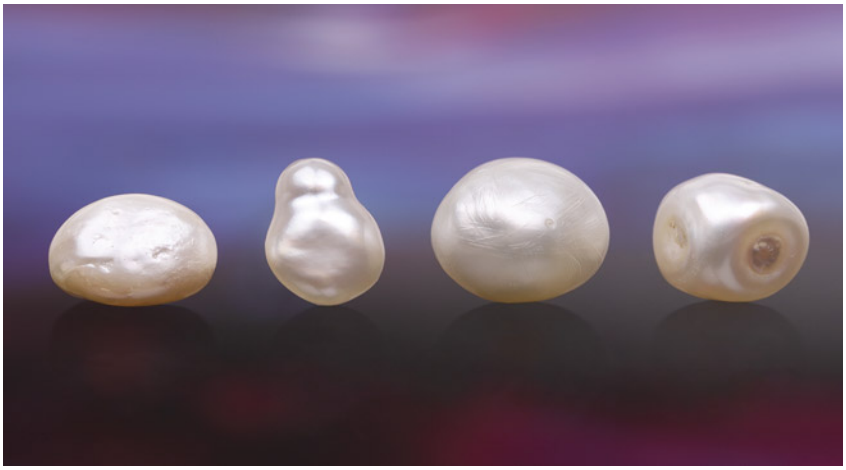

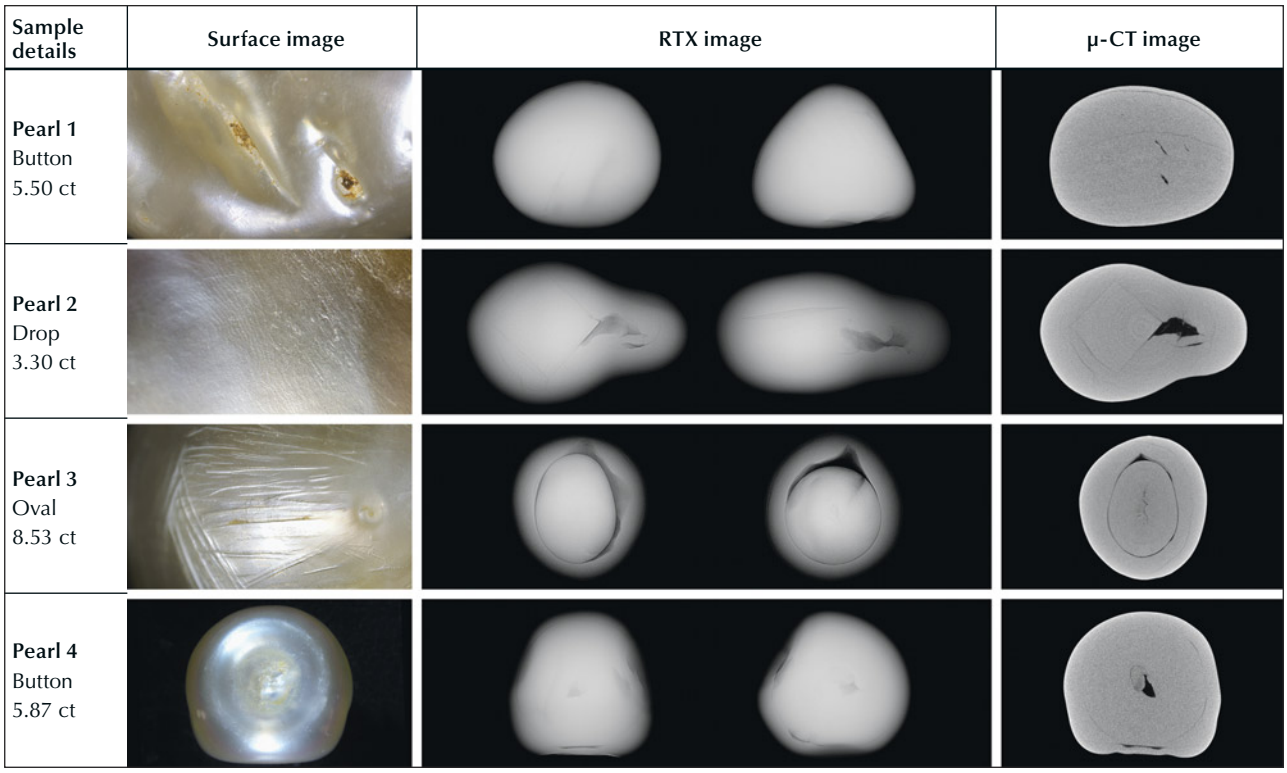

Figure 8. Surface appearance and internal structures of the four atypical bead cultured pearls. Fields of view 2 mm, 0.6 mm, 2.86 mm, and 16.3 mm.

the surface which was not continuous. On viewing the μ-CT, the demarcation was more discernible and followed the irregular outline of the pearl (figure 8, row 1). An irregularly shaped freshwater shell bead was clearly used as the nucleus, hence the strong yellowish green reaction observed in the optical X-ray fluorescence unit (figure 9, left). Under transmitted light, banding within the bead nucleus was also observed (figure 9, right); externally, the pearl had notable indentations on its surface.

Pearl 2 hosted the most interesting nucleus of the four. A rectangular "tissue-box" shaped bead, likely a piece of cut saltwater shell given the almost identical radio-opacity to that of its host, was evident in the RTX and μ-CT images (figure 8, row 2) (Fall 2022 Gem News International, pp. 378–380). Externally, the pearl was smooth, lustrous, and free of any surface blemishes.

The RTX and μ-CT images of pearl 3 revealed an obvious demarcation with a linear structure at the center of the nucleus and a small "organic tail-like feature" at one end within the boundary separating the bead from the overgrown cultured nacre (figure 8, row 3). All features were consistent with a saltwater non-bead cultured pearl being used as the bead nuclei. The lack of growth arcs around the demarcation was possibly due to rapid nacre deposition during the culturing process ("Atypical 'beading' in the production of cultured pearls from Australian *Pinctada maxima*," *GIA Research News*, February 13, 2017). This pearl exhibited distinct surface scratches that were visible without magnification.

Pearl 4 also showed a strong demarcation feature on the RTX and μ-CT images. However, the central area

Figure 9. Left: Pearl 1 revealed a strong yellowish green reaction under optical X-ray fluorescence. Right: Undulating shell banding visible within the sample's shell bead nucleus using transmitted light; field of view 6.75 mm.

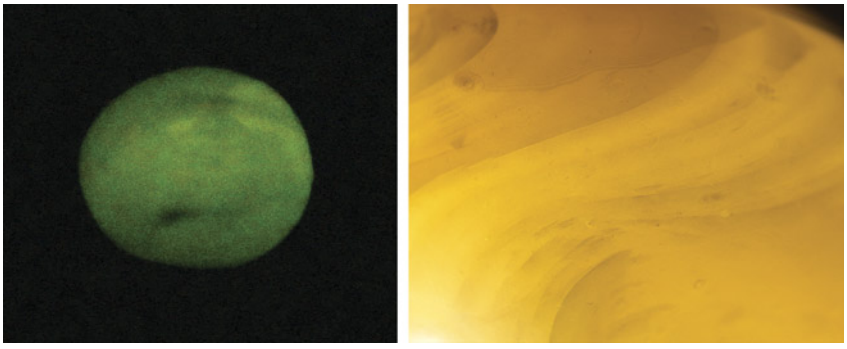

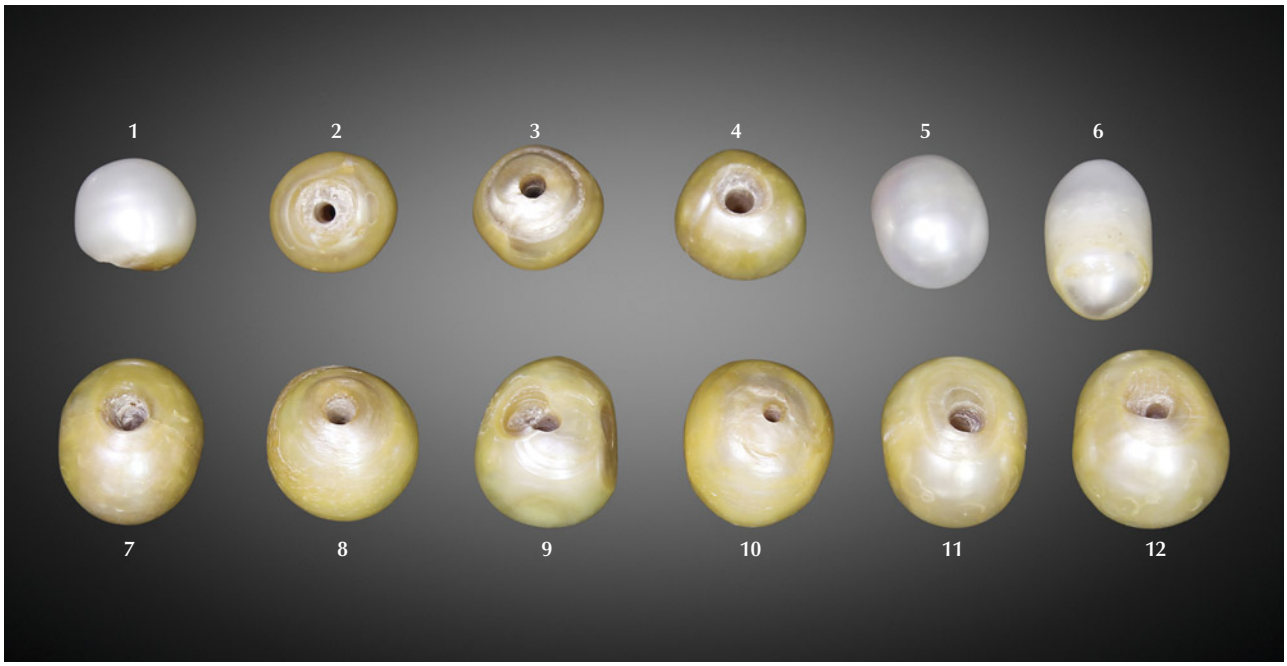

Figure 10. A group of 12 pearls ranging from 7.38 × 6.49 × 6.05 mm to 10.61 × 9.05 × 8.05 mm and weighing 44.37 carats total.

differed from the other three pearls, as it showed a void-like feature in the middle (figure 8, row 4). The bead nucleus used in the process was most likely a saltwater non-bead cultured pearl based on the fact that the pearl was inert to XRF, in keeping with pearl 3, despite the relatively thin nacre layers that would allow a freshwater bead to react. The pearl was also unusual because it possessed three nearly flat "bases" with concave features at the center of each. This raised questions about its identity even before X-ray examination, since the authors have rarely observed natural pearls with such features.

This is not the first time GIA has encountered aBCPs, but to receive four with variations on two types of nuclei—atypical shell (not typical round shell beads) and non-bead cultured pearls—in one lot was very interesting. This proves that such pearls are still circulating in the market and are being mixed with natural goods in an attempt at deception (Fall 2011 Lab Notes, pp. 229–230). Given the spectral data collected (S. Karampelas, "Spectral characteristics of natural-color saltwater cultured pearls from *Pinctada maxima*," Fall 2012 *G&G*, pp. 193–197) and the pearls' internal structures and external appearance (A. Homkrajae et al., "Internal structures of known *Pinctada maxima* pearls: Cultured pearls from operated marine mollusks," Fall 2021 *G&G*, pp. 186–205), it is apparent that all four of them formed within *Pinctada* species mollusks, most likely *Pinctada maxima*. Atypical bead cultured pearls have always been an interesting and sometimes challenging subject. With modern equipment and practical pearl testing experience, laboratories such as GIA aim to remain one step ahead of the possible experiments used by cultivators.

Rajesh S. Patel, Abeer Al-Alawi, Lubna Sahani, and Nicholas Sturman

Treated Freshwater Non-Bead Cultured Pearls with an Antique Appearance

GIA's Mumbai laboratory recently received for identification a group of nine drilled and three undrilled pearls weighing 44.37 carats total and ranging in size from 7.38 × 6.49 × 6.05 mm to 10.61 × 9.05 × 8.05 mm. The nine drilled pearls appeared to be old, while the three undrilled pearls looked whiter and much newer overall (figure 10). The shape of the samples varied, and the nine drilled pearls possessed a notable "aged" yellow coloration, which was also evident on some areas of the three undrilled whiter pearls.

The older-looking pearls possessed a dull luster, but the nacre condition was good. Microscopic examination at 70× magnification soon revealed that the color was concentrated on the outer layers and within surface-reaching features, proving that the color was not natural and a treatment had been used to alter their appearance (Summer 2017 Gem News International, pp. 255–256).

Although the color of pearls can change over time due to various causes (e.g., care factors such as storage conditions and contact with chemicals), these changes tend to be very gradual and develop over many years. This is partly due to their bio-

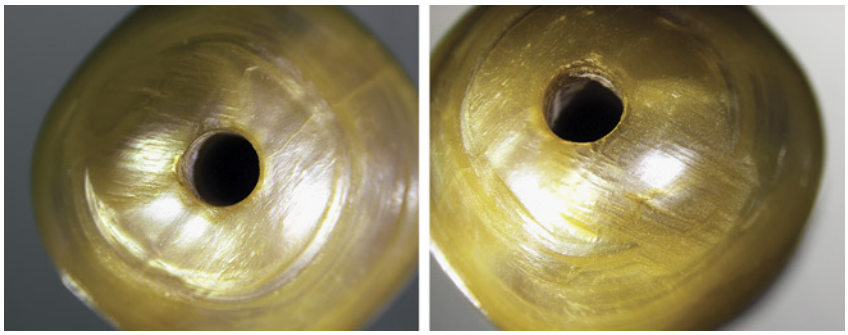

Figure 11. Two of the samples showing uneven surface coloration and color concentrations around the large drill holes. The worked surfaces around the drill holes are also clearly visible. Field of view 6.00 mm.

genic composition, which mainly consists of calcium carbonate with traces of organic substances, residual substances, and water. Dry environments are generally not advisable as they may result in surface alterations and, in rare cases, weight loss. The color can also change over time through wear and tear and the accumulation of external contaminants, so further analysis was required to prove whether these pearls naturally discolored over time or were treated to look antique, thereby inflating their value (M.S. Krzemnicki, "Fake historic provenance: 'Aged' cultured pearls," *Facette*, No. 25, 2019, p. 28).

Visually, it was readily apparent that the drill holes were very large in relation to the size of the pearls. When viewed with a 10× lens or under a gemological microscope at 70×, color concentrations were observed around the drill holes of all nine drilled pearls. The surfaces were also heavily worked around the drill holes and did not resemble the wear and tear that might be expected on antique pearls. The surfaces of the nine drilled samples (2–4 and 7–12) were also slightly etched, indicating possible exposure to a mild acidic solution to create an "aging" effect.

Figure 12. An area of underlying white color below the treated surface of one of the samples. Field of view 5.00 mm.

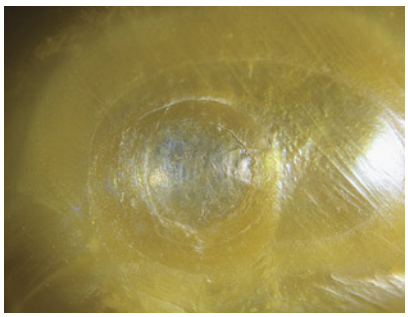

Strikingly, the color was not typical of natural-color pearls (Summer 2017 Gem News International, pp. 255–256) and appeared to be restricted to the surface and around the drill holes (figure 11). Areas on some pearls also revealed the original underlying white color, further proof of treatment (figure 12).

Next, we needed to determine whether the pearls originated from a saltwater or freshwater environment, and whether they were natural or cultured. Real-time microradiography revealed small central twisting void-like features surrounded by fine growth lines typical of freshwater non-bead cultured pearls (figure 13), consistent with those produced by Chinese farms (K. Scarratt et al., "Characteristics of nuclei in Chinese freshwater cultured pearls," Spring 2000 *G&G*, pp. 98–109). The freshwater origin was confirmed when the pearls fluoresced a strong yellowish green color upon exposure to X-ray fluorescence, and further substanti-

Figure 13. The internal structures of four of the pearls showed twisted void-like features surrounded by fine growth arcs characteristic of non-bead cultured freshwater pearls. The two wide vertical gray features seen in pearls 3 and 4 are the drill holes.

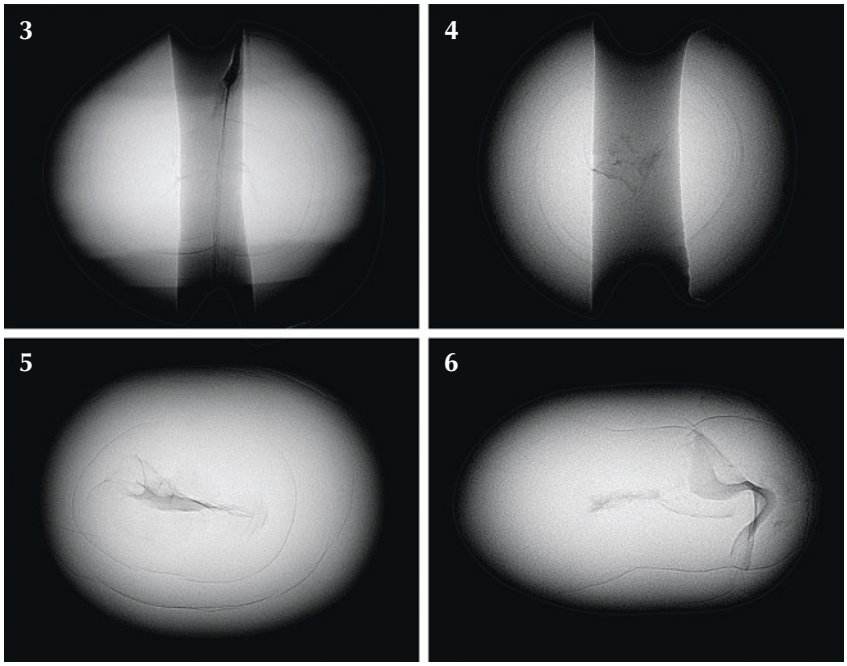

ated by manganese values ranging from 500 to 1700 ppm and strontium values from 800 to 1000 ppm, obtained by energy-dispersive X-ray fluorescence spectroscopy.

Since Raman spectroscopy is also a valuable analytical tool for differentiating natural versus treated color in pearls, 514 nm ion-argon laser excitation was used on the surfaces. The results revealed a doublet at 702 and 705 cm^{-1}, as well as a peak at 1085 cm^{-1} indicative of aragonite, which is seen in the majority of pearls. High background fluorescence, often characteristic of treated-color pearls, was also noted in the drilled pearls. The photoluminescence spectra obtained displayed high fluorescence more typical of treated pearls, as well as the expected aragonite peaks. Other than the suspiciously high fluorescence, no other peaks characteristic of dyeing were observed.

All observations and results indicated that the nine drilled pearls had been treated to make them look antique. Pearls 1, 5, and 6 were predominantly white and showed only minimal evidence of any artificial aging attempts. These three showed a reaction to long-wave UV fluorescence more indicative of routine processing carried out on freshwater pearls. We concluded that these freshwater non-bead cultured pearls were also treated to make them appear aged. Hence, the report stated that these were freshwater non-bead cultured pearls from the Unionidae family and that pearls 2–4 and 7–12 had been color modified. Since the majority of the surfaces of pearls 1, 5, and 6 remained white and only showed insignificant areas of discoloration, the modified color description was not applied.

Andrew Aron, Abeer Al-Alawi, and Nicholas Sturman

Heart-Shaped Golden South Sea Cultured Pearl

The heart shape has been a worldwide symbol of love and romance for centuries. GIA's New York laboratory recently received a golden-colored heart-shaped pearl pendant that drew our attention. The pearl was reportedly produced in the Philippines, which is a major source of golden South Sea cultured pearls. Upon routine gemological and advanced instrumental examination—including microradiography, ultraviolet/visible spectroscopy, manganese and strontium contents from energy-dispersive X-ray fluorescence, and reaction to long-wave UV—we concluded that it was an atypical bead cultured pearl from the *Pinctada maxima* species, commonly known in the trade as a South Sea cultured pearl (figure 14), and its heart shape and golden color were entirely natural.

Figure 14. A heart-shaped golden South Sea pearl pendant measuring 17.78 × 11.65 × 9.07 mm and weighing 1.93 g (including the 18K yellow metal findings).

Unlike the traditional bead cultured pearls typically nucleated with spherical shell bead nuclei, a heart-shaped bead nucleus was used in this pearl to achieve its unique shape. Hence, it was described as an "atypical bead" cultured pearl (aBCP) according to GIA's pearl identification terminology. Real-time microradiography (RTX) and X-ray computed microtomography (CT) clearly revealed the internal structure of a heart-shaped bead nucleus (figure 15). The nacre coverage, averaging 0.80 mm thick, was evenly distributed all around the nucleus, demonstrating that the heart shape of the pearl was consistent with the shape of the nucleus. Magnification revealed no signs of surface working or treatment, suggesting the pearl was in its original form after harvest. It displayed a strong orangy yellow color that is highly sought after among South Sea pearls. Ultraviolet/visible reflectance and photoluminescence spectroscopy further confirmed its natural color origin (C. Zhou et al., "Update on the identification of dye treatment in yellow or 'golden' cultured pearls," Winter 2012 *G&G*, pp. 284–291).

Although this was not the first time a heart-shaped pearl has been examined in the lab, it is very rare to see a whole pearl with such a perfect non-round cultured shape. Previous submissions have either been identified as mabe pearls (assembled cultured blisters) or have had poorly defined heart shapes. Mabe pearls are not con-

Figure 15. X-ray images from RTX (left) and CT (right) show the demarcation of a heart-shaped bead nucleus with an average nacre thickness of 0.80 mm.

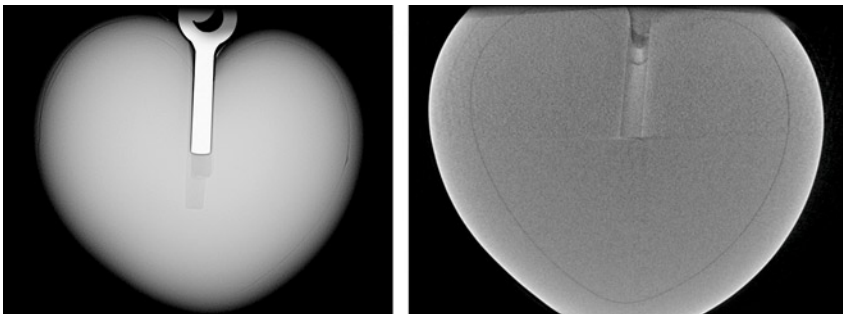

sidered whole pearls and often possess a thin nacre dome top (Fall 2021 Gem News International, pp. 277–279). Due to the thin nacre, their shape is easier to control. Therefore, fancy-shaped nuclei are commonly used in mabe pearls.

Many atypical bead cultured pearls have been studied and examined over the years at GIA ("Atypical 'beading' in the production of cultured pearls from Australian *Pinctada maxima*," *GIA Research News*, February 13, 2017; Fall 2022 Gem News International, pp. 378–380). However, the majority of the end products are very different from the original shape of the nuclei. This remarkable use of an atypical bead nucleus to achieve a perfect shape in a cultured pearl suggests recent improvements in pearl culturing techniques.

Joyce Wing Yan Ho and Emiko Yazawa

Figure 16. The natural shell blister attached to a portion of the shell on which it formed, weighing 2.60 g (13.00 ct) total and measuring 25.54 × 18.11 × 7.79 mm.

A Gastropod Shell in a Unique Shell Blister

Natural blister pearls and natural shell blisters have long been a subject of debate for gemologists and can be very challenging to definitively identify (see *G&G* Lab Notes from Fall 1992, Spring 1995, Winter 1996, Winter 2015, Summer 2016, and Spring 2018). According to the World Jewellery Confederation (CIBJO), a natural blister pearl forms when a natural pearl detaches itself from the pearl sac and attaches to the inner wall of the shell, while a natural shell blister is an internal protuberance that forms on a shell's inner surface. It is usually caused by a foreign object accidentally finding its way into the space between the mantle and shell surface.

GIA's Mumbai laboratory recently examined an interesting dark greenish brown baroque-shaped blister attached to a portion of shell weighing 2.60 g (13.00 ct) total and measuring approximately 25.54 × 18.11 × 7.79 mm (figure 16).

Examination under 40× magnification revealed a graduated hexagonal structure on the shell base (figure 17, A and B). The shell was cut and worked around the edges, and growth layers were visible when the cut surfaces were examined. Exposure to X-ray fluorescence yielded no reaction for the shell blister. Energy-dispersive X-ray fluorescence spectrometry on two areas (top and base) revealed manganese levels below the detection limit, and strontium levels of 1470 ppm (top) and 2431 ppm (base) were consistent with those expected for saltwater pearls.

Figure 17. Photomicrographs show graduated cellular structures from the natural shell blister examined in the Mumbai laboratory (A and B; fields of view 4 mm and 3 mm, respectively) compared to those from a known Pinnidae shell from GIA's Bangkok laboratory (C and D; fields of view 4 mm and 3 mm, respectively).

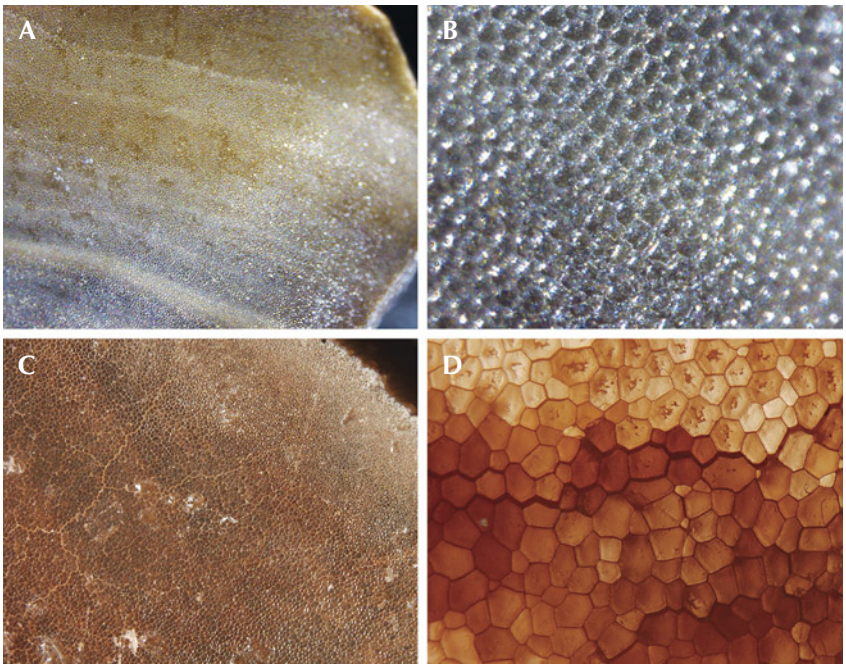

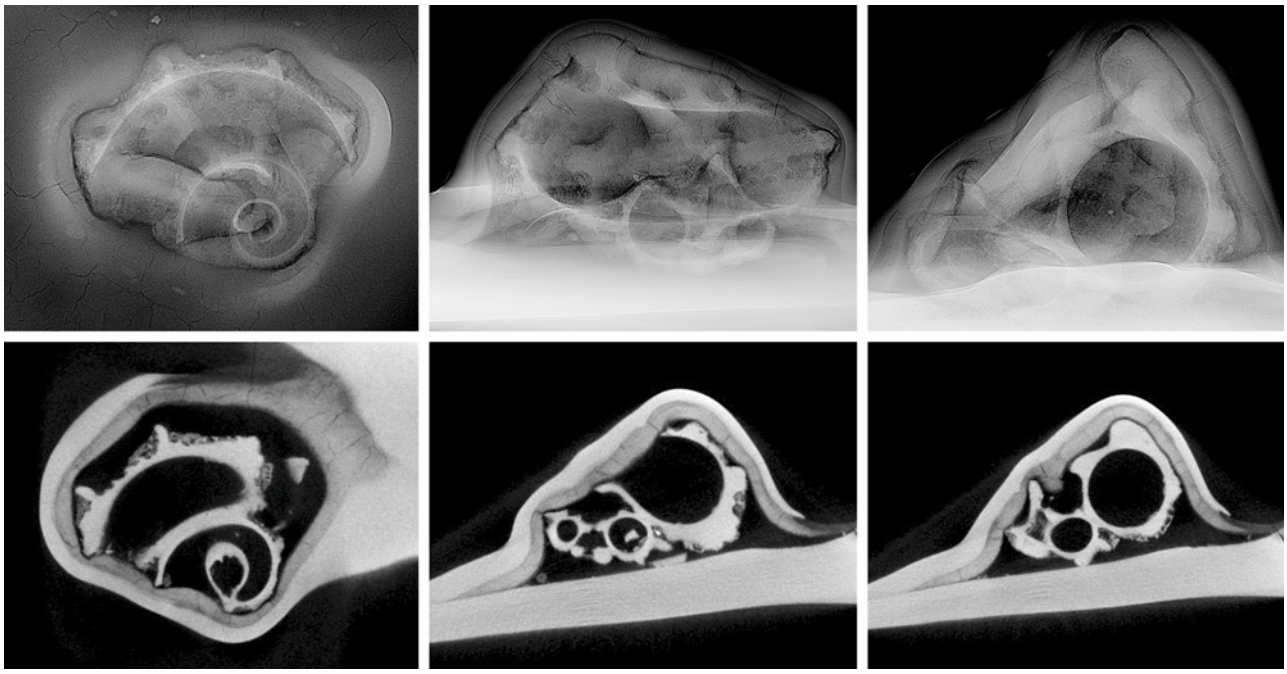

Figure 18. Top row, left to right: RTX images of the face, the right side, and the length or thickest direction reveal a prominent gastropod shell measuring approximately 8.30 × 5.75 mm within the shell blister. Bottom row: µ-CT images show the structures for the same three directions and provide even clearer details of the entombed gastropod.

Real-time microradiography (RTX), shown in the top row of figure 18, revealed a pleasant surprise. An obvious and intriguing gastropod shell was hidden beneath the overlying layers, which resulted in further study using X-ray computed microtomography (µ-CT) (figure 18, bottom row). The minute details of a unique marine gastropod exoskeleton measuring approximately 8.30 × 5.75 mm were observed within a void feature, and the overlying growth layers on the face side (the surface that grew within the mollusk it formed in) revealed minimal growth arcs. Marine gastropods are known to vary in size, and the class consists of many thousands of species (A. Nutzel., "Larval ecology and morphology in fossil gastropods," *Paleontology*, Vol. 57, No. 3, 2014, pp. 479–503). These observations provided enough evidence to make a clear distinction between a shell blister, such as this sample, and a shell blister pearl ("Natural shell blisters and blister pearls: What's the difference?" *GIA Research News*, August 26, 2019).

The ultraviolet/visible reflectance spectra showed a prominent feature at around 450 nm and weaker features at 320, 330, 450, and 460 nm proving that the sample's color was natural and lacked any treatment. Raman analysis using 514 nm laser excitation showed a series of peaks at 158, 186, 204, and 213 cm^{-1}; a weak peak at 280 cm^{-1}; a doublet peak around 701–704 cm^{-1}; and a strong peak at 1085 cm^{-1}. These were indicative of aragonite. The photoluminescence spectra were also consistent with the Raman and displayed high fluorescence and aragonite-related peaks. These results were unexpected given the cellular-looking structure observed through the microscope, as this type of structure usually results in Raman spectra indicative of calcite.

While the lustrous dark color and the cellular-looking structure indicated the host shell was likely a species from the Pinnidae family, it was not clear given the spectral data collected (N. Sturman et al., "Observations on pearls reportedly from the Pinnidae family (pen pearls)," Fall 2014 *G&G*, pp. 202–215). When the surface structures were compared to photomicrographs of known *Pinna* species shell from GIA's Bangkok laboratory (figure 17, C and D), the results showed some similarity. However, Raman spectra indicative of calcite were obtained for the Bangkok research collection samples, which differed from the sample studied here. The *Atrina vexillum* species may have been responsible for producing the natural shell blister, and this would explain the aragonite-related Raman peaks since this mollusk is known to produce pearls with an aragonitic structure. However, since *Atrina* species pearls are often nacreous when aragonite is present and the sample in question was non-nacreous, the contradicting data still leaves some doubt as to the true identity of the host. Nevertheless, this example of a shell blister encompassing a gastropod shell represents a noteworthy phenomenon of nature that is rarely encountered.

Jayesh Surve, Abeer Al-Alawi, and Nicholas Sturman

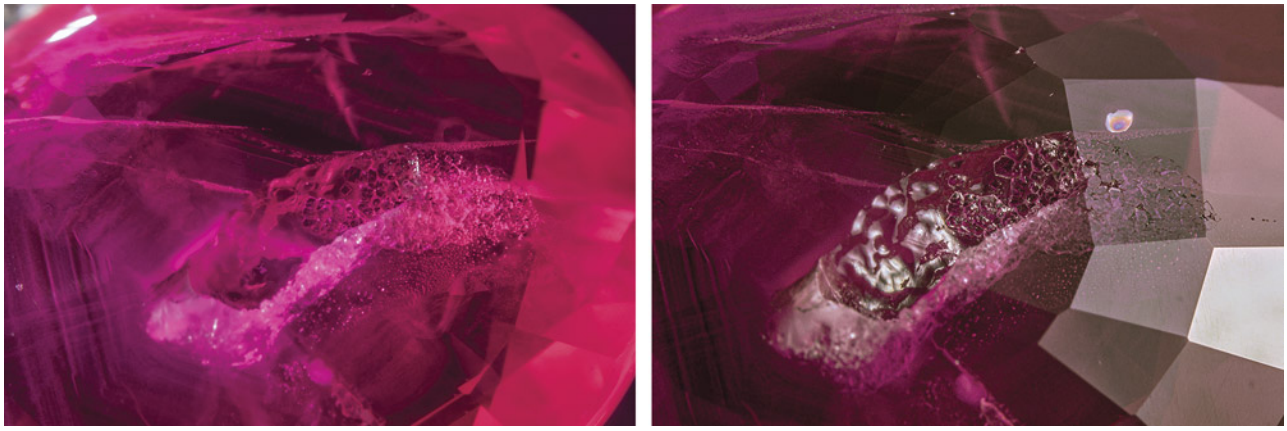

Figure 19. A large cavity partially filled with synthetic overgrowth on the pavilion of a heated Burmese ruby in darkfield lighting (left) and reflected lighting (right). Field of view 7.19 mm.

RUBY with Interesting Synthetic Overgrowth

The Carlsbad laboratory received a 3.02 ct ruby for a colored stone identification and origin report. Standard gemological testing was consistent with ruby: a hydrostatic specific gravity of 3.96 and a ruby spectrum in a handheld spectroscope. Internally, the stone displayed white flakes in a hexagonal formation and roiled graining. Partially healed fissures with residue, which result from heating in the presence of a flux, were also documented. The inclusion scene, along with the stone's trace element chemistry collected using laser ablation–inductively coupled plasma–mass spectrometry (LA-ICP-MS), were consistent with Burmese ruby. This ruby was not treated by beryllium diffusion, as no beryllium was detected by LA-ICP-MS. The curious feature of this stone was a large cavity on the pavilion that was partially filled with synthetic overgrowth that was observed in the microscope (figure 19).

Synthetic overgrowth can be a byproduct of heating a piece of corundum at high temperatures, with or without the presence of a flux. This creates an environment in the crucible that allows for the partial dissolution of corundum and can result in synthetic corundum overgrowth on the surface and in cavities of the heated stone. Synthetic overgrowth is typically an aggregated structure of hexagonally shaped, platy crystals (Fall 2002 *G&G* Lab Notes, pp. 255–256). When viewed in reflective lighting, there is no luster difference between the host corundum and the synthetic overgrowth, as the two materials have the same refractive index. The gaps that could be observed between the crystals in this stone showed how they grew in different orientations.

Synthetic overgrowth is common enough that it should always be looked for in corundum that has undergone high-temperature heat treatment. There are cases where synthetic overgrowth can be observed using polarized light, but careful analysis is required because the overgrowth can completely fill cavities and be inconspicuous.

Nicole Ahline

Exceptionally Large SYNTHETIC RUTILE

The Carlsbad laboratory received three light yellow modified round brilliants weighing 11.13, 11.91, and 110.18 ct (figure 20) for identification reports. Standard gemological testing revealed the stones to be synthetic rutile based

Figure 20. Three large synthetic rutile brilliants weighing 11.13, 110.18, and 11.91 ct. Courtesy of Arya Akhavan.

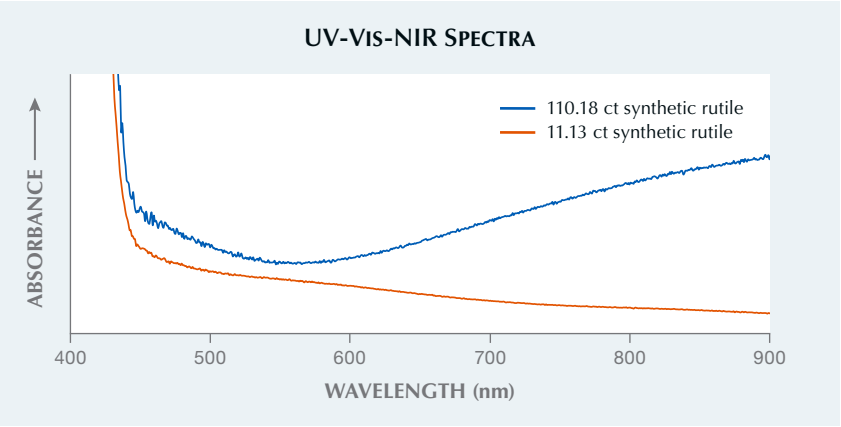

Figure 21. UV-Vis-NIR absorption spectra comparing the 110.18 ct and 11.13 ct synthetic rutile studied, here demonstrating the effect of aluminum doping in the smaller stone to produce a nearly colorless appearance.

on over-the-limit refractive index readings and extreme fire and doubling, an identification that was supported by Raman spectroscopy.

Of particular note was the astonishing size of these stones. The 110.18 ct synthetic rutile is the largest encountered in the GIA laboratory. Even the smaller 11.13 ct and 11.91 ct stones are much larger than normal for this material, which is usually seen in sizes up to several carats. The owner of the stones indicated that the manufacturer had to modify their furnace to accommodate growth of the 110.18 ct crystal. Also notable were the novel facet pattern and precision cutting usually only seen in the high-end collector market.

Interestingly, the two smaller stones had a much lighter yellow color than the 110.18 ct stone, which was notable even considering the shorter light path length through the smaller stones. Chemical analysis using laser ablation–inductively coupled plasma–mass spectrometry showed a higher concentration of aluminum in these two samples (~80 ppm Al compared to ~3 ppm). The difference in color was also demonstrated in the ultraviolet/visible/near-infrared absorption spectra (figure 21). This finding aligns with the practice of growing rutile doped with small amounts of aluminum to bring the appearance of the material closer to nearly colorless (C.H. Moore, "Rutile boule and method of making the same," U.S. Patent 2,715,070, issued August 9, 1955). Additionally, the owner indicated that the two smaller rutile crystals were grown by National Lead Co. between 1961 and 1964, while the larger stone is from a modern producer.

Aaron Palke

PHOTO CREDITS
Adrianna Gudino—1; Nathan Renfro—2; Towfiq Ahmed—3; Johnny Leung–4; Sze Ling Wong—5, 6; Gaurav Bera—7, 16; Nishka Vaz—8, 9 (right); Jayesh Surve—10–12, 17 (A and B); Sood Oil (Judy) Chia—14; Nicholas Sturman—17 (C and D); Nicole Ahline—19; Robert Weldon—20